Title

Pulmonary Lymphangiectasia Resulting From Vascular Endothelial Growth Factor-C Overexpression During a Critical Period

Journal

Circulation Research, 114(5)

ISSN

0009-7330

Authors

Yao, Li-Chin
Testini, Chiara
Tvorogov, Denis
et al.

Publication Date

2014-02-28

DOI

10.1161/circresaha.114.303119

Peer reviewed

Published in final edited form as:
Circ Res. 2014 February 28; 114(5): 806–822. doi:10.1161/CIRCRESAHA.114.303119.

Pulmonary Lymphangiectasia Resulting from Vegf-C Overexpression During a Critical Period

Li-Chin Yao[1], **Chiara Testini**[2], **Denis Tvorogov**[3], **Andrey Anisimov**[3], **Sara O. Vargas**[4], **Peter Baluk**[1], **Bronislaw Pytowski**[5], **Lena Claesson-Welsh**[2], **Kari Alitalo**[3], and **Donald M. McDonald**[1]

[1]Cardiovascular Research Institute, Comprehensive Cancer Center, and Department of Anatomy, University of California, San Francisco, California, USA [2]Department of Immunology, Genetics and Pathology, Rudbeck Laboratory, Uppsala University, Uppsala, Sweden [3]Wihuri Research Institute and Translational Cancer Biology Program, Biomedicum, Helsinki and University of Helsinki, Finland [4]Department of Pathology, Boston Children's Hospital, Harvard University, Massachusetts, USA [5]Department of Cell Biology, ImClone Systems, Eli Lilly and Company, New York, New York, USA

Abstract

Rationale: Lymphatic vessels in the respiratory tract normally mature into a functional network during the neonatal period, but under some pathological conditions can grow as enlarged, dilated sacs that result in the potentially lethal condition of pulmonary lymphangiectasia.

Objective: We sought to determine whether overexpression of the lymphangiogenic growth factor VEGF-C can promote lymphatic growth and maturation in the respiratory tract. Unexpectedly, perinatal overexpression of VEGF-C in the respiratory epithelium led to a condition resembling human pulmonary lymphangiectasia, a life-threatening disorder of the newborn characterized by respiratory distress and the presence of widely dilated lymphatics.

Methods and Results: Administration of doxycycline to CCSP-rtTA/tetO-VEGF-C double transgenic mice during a critical period from E15.5 to P14 was accompanied by respiratory distress, chylothorax, pulmonary lymphangiectasia, and high mortality. Enlarged sac-like lymphatics were abundant near major airways, pulmonary vessels, and visceral pleura. Side-by-side comparison revealed morphologic features similar to pulmonary lymphangiectasia in humans. The condition was milder in mice given doxycycline after age P14 and did not develop after P35. Mechanistic studies revealed that VEGFR-3 alone drove lymphatic growth in adult mice, but both VEGFR-2 and VEGFR-3 were required for the development of lymphangiectasia in neonates. VEGFR-2/VEGFR-3 heterodimers were more abundant in the dilated lymphatics, consistent with the involvement of both receptors. Despite the dependence of lymphangiectasia on VEGFR-2 and VEGFR-3, the condition was not reversed by blocking both receptors together or by withdrawing VEGF-C.

Conclusions: The findings indicate that VEGF-C overexpression can induce pulmonary lymphangiectasia during a critical period in perinatal development.

Address correspondence to: Dr. Donald M. McDonald Department of Anatomy 513 Parnassus Ave. Room S-1349 University of California- San Francisco San Francisco, CA 94143 Tel: 415-476-2118 Fax: 415-476-4845 donald.mcdonald@ucsf.edu.

DISCLOSURES

Bronislaw Pytowski is an employee of ImClone Systems, Eli Lilly and Company. Other authors have no conflicts of interest to declare.

Keywords

Chylothorax; Clara cells; lung; lymphatic capillary; lymphatic malformations; lymphangiogenesis; lymphangiomatosis; VEGFR-2; VEGFR-3; proximity ligation assay; pulmonary edema

INTRODUCTION

Lung lymphatics serve as routes for transport of extracellular fluid, antigens, and immune cells to lymph nodes [1, 2], but this can change in conditions where lymphatics regress, overgrow, or otherwise become dysfunctional [3]. Congenital pulmonary lymphangiectasia is a life-threatening developmental disorder where newborn infants have respiratory distress, cyanosis, pleural effusion or chylothorax, and widely dilated lymphatics in the lung [4-6]. From the initial description more than 150 years ago by Rudolf Virchow [7] and many subsequent reports [8-11], pulmonary lymphangiectasia is distinguished by the presence of large lymphatic sacs, cysts, or networks around major bronchi and pulmonary blood vessels, within interlobular septa, and beneath the visceral pleura. For many years, most babies with the condition were stillborn or died soon after birth. Improvements in neonatal intensive care have led to better outcomes in some cases [12], but many still succumb. Pulmonary lymphangiectasia can occur in patients with congenital heart disease, can accompany chromosomal disorders such as Noonan syndrome and Down syndrome, or can have a late onset in older children [6, 10, 13]. Lymphangiectasia can also occur in extrapulmonary sites including the intestine, pancreas, heart, kidneys or in multiple organs [8, 14-16].

The etiology of pulmonary lymphangiectasia is unknown, and no disease-specific therapies or animal models have been developed. Among the factors that could contribute to the condition, defective signaling of the lymphangiogenic factor VEGF-C through its receptor VEGFR-3 is a likely candidate. Activation of VEGFR-3 signaling by VEGF-C is essential for normal development of the lymphatic vascular system [17] and can promote growth of lymphatics in the adult [18-20]. After proteolytic processing to the mature protein, VEGF-C can also activate VEGFR-2 [21], which drives lymphangiogenesis under some conditions [22, 23]. VEGF-D, the other known ligand for VEGFR-3, appears to be dispensable because lymphatic development proceeds normally in its absence [24] but can substitute when VEGF-C is not present [25].

Lymphangiogenesis is a feature of sustained inflammation of the airways and lung [20, 26] and occurs in multiple other lung conditions [3]. Despite the abundance of lymphatics accompanying inflammation, leaky blood vessels lead to airway mucosal edema, perhaps because the new lymphatics are immature, abnormal, or dysfunctional and unable to handle the fluid load [20, 27, 28]. Lymphatic dysfunction in these pathological conditions contrasts with lymphatic growth promoted by engineered overexpression of VEGF-C, which can increase lymph flow and reduce inflammatory responses in skin and joints [29, 30].

We sought to determine whether switching on VEGF-C to drive lymphatic growth in the respiratory tract before the onset of inflammation could ameliorate subsequent inflammatory responses. To our surprise, activation of VEGF-C overexpression in neonatal mice – but not in adults - led to a condition resembling pulmonary lymphangiectasia. This growth of lymphangiectatic vessels differed from reported effects of VEGF-C overexpression in skin and joints [19, 29, 30]. It also differed from reported effects of VEGF-A overexpression in the airway and lungs, where the new blood vessels grow as tubular sprouts, not as sheets, sacs, or cystic structures [31, 32].

This unanticipated finding provided the opportunity to obtain a better understanding of how lymphangiectasia develops in the respiratory tract. We reasoned that the finding of lymphatics growing as irregular sheets or bags instead of simple tubes after overexpression of VEGF-C in the respiratory tract could provide insights relevant to human pulmonary lymphangiectasia. We therefore examined the development, mechanism and reversibility of lymphangiectasia in the airways and lung of CCSP-rtTA/tetO-VEGF-C double transgenic mice in which VEGF-C expression was driven by the promoter of Clara cell secretory protein (CCSP) under doxycycline regulation. We learned that pulmonary lymphangiectasia developed in these mice only when VEGF-C overexpression occurred during a critical period from embryonic day 15.5 (E15.5) to postnatal day 14 (P14). Development of lymphangiectasia required VEGF-C signaling through both VEGFR-2 and VEGFR-3 and involved the formation of VEGFR-2/VEGFR-3 heterodimers, unlike lymphangiogenesis in the adult that required only VEGFR-3. Once lymphangiectasia developed, the abnormal lymphatics resisted regression, even after inhibition of VEGFR-2/VEGFR-3 signaling by function blocking antibodies or withdrawal of VEGF-C.

METHODS

Mice

We generated CCSP-rtTA; tetO-VEGF-C double-transgenic mice (designated CCSP-VEGF-C mice) by breeding mice of the Clara cell secretory protein reverse tetracycline transactivator (CCSP-rtTA) driver line (The Jackson Laboratory, strain #006222, line 1) [33] with mice of the tetracycline operator (tetO)-mVEGF-C responder line [19]. In CCSP-rtTA driver mice, doxycycline induces rapid, reversible expression of full-length mouse VEGF-C in Clara cells and alveolar type II cells of the respiratory epithelium [34]. In tetO-VEGF-C responder mice, lymphangiogenesis is driven by VEGF-C overexpressed in the target cells, as previously shown in skin [19]. Some transgenic mice were crossed with Prox1-GFP mice [35] to make triple transgenic mice with green fluorescent lymphatics. Double transgenic mice without doxycycline, which had no apparent phenotype, were used as controls. All mice were pathogen-free and were housed under barrier conditions. Before being subject to experimental procedures, mice were anesthetized by intramuscular injection of ketamine (87 mg/kg) and xylazine (13 mg/kg). Each experimental group had 8 to 10 mice. All experiments were approved by the Institutional Animal Care and Use Committee of the University of California at San Francisco.

Human specimens

Human lung specimens obtained at autopsy (Case A) or by wedge biopsy (Cases B and C) were fixed in formalin, embedded in paraffin, sectioned at a thickness of 5 μm, and stained with hematoxylin and eosin (H&E) or by immunohistochemistry (see Supplemental Methods). The Institutional Review Board of Boston Children's Hospital approved the study and waived the need for individual patient consent because it was restricted to a retrospective review of slides and reports and met the other institutional standards including next-of-kin consent for autopsy, parent/guardian consent for biopsy, patient confidentiality protections, and other requirements.

Doxycycline administration

To activate VEGF-C expression, CCSP-VEGF-C mice received doxycycline (Sigma-Aldrich) at a concentration of 0.001 to 5 mg/ml in drinking water containing 5% sucrose [36]. CCSP-VEGF-C littermates on normal water were used as controls, unless described otherwise. In some experiments, mice received doxycycline by ip injection at a dose of 100 μg/g every other day (see Supplemental Methods). In reversal studies, VEGF-C expression was turned off by removing doxycycline from drinking water.

Inhibition of VEGFR-2 and/or VEGFR-3 signaling

Function-blocking, rat monoclonal antibodies were administered to inhibit signaling of VEGFR-2 (DC101) and/or VEGFR-3 (mF4-31C1) (ImClone/Eli Lilly, New York). Antibodies were injected ip at an initial dose of 100 μg/g and then 40 μg/g every other day [20]. Control mice received sterile 0.9% NaCl, which was previously found to be indistinguishable from control rat IgG in this setting [28]. In prevention studies, mice were given the inhibitory antibodies and doxycycline concurrently for 7 days. In reversal studies, doxycycline was given for 7 days, and then the antibodies were given for the next 7 days without doxycycline.

Preparation of mouse tissues

Tissues were fixed by vascular perfusion of fixative (1% paraformaldehyde in PBS, PH 7.4) through the pulmonary artery via the right ventricle, at a pressure of 20-40 mmHg until the lungs turned white, and then perfusion via the left ventricle for 2 min at 120-140 mmHg. Trachea, lungs, diaphragm, mesentery, and skin from the ventral midline of the abdomen were prepared as whole mounts for immunohistochemical staining (see Supplemental Methods) [28]. Some tissues were embedded in OCT (Sakura Finetek) and cryosectioned or embedded in paraffin, sectioned, and stained with H&E.

In situ proximity ligation assay (PLA)

Cryostat sections of trachea 10 μm in thickness were mounted on slides, stained for LYVE-1 immunoreactivity (AngioBio, rabbit polyclonal), and incubated with secondary antibody anti-rabbit Alexa 488 (Jackson ImmunoResearch). Slides were then subjected to in situ PLA using Duolink kits (Olink Bioscience, Uppsala, Sweden) according to the manufacturer's instructions [37]. Sections were incubated overnight with primary antibodies to VEGFR-2 (Cell Signaling, rabbit anti-mouse, clone 55B11) and VEGFR-3 (R&D, goat polyclonal, #AF743) followed by incubation with secondary antibody-conjugated PLA probes (anti-rabbit PLUS, #LNK-92002, and anti-goat MINUS, #LNK-92006, Axxora, NY) for one hour at 37°C. After the ligation and rolling circle amplification (RCA) steps, the single-strand RCA products were hybridized by 554-nm fluorophore-conjugated complementary oligonucleotides (Duolink In Situ Detection Reagents Orange). VEGFR-2/VEGFR-3 heterodimers visible as bright red fluorescent dots were imaged by confocal microscopy with a Cy3 filter. The number of PLA dots per lymphatic endothelial cell, defined as DAPI-stained nucleus colocalized with LYVE-1, was counted in 5 sections per mouse ($N = 3$ per group). As controls, each primary antibody was omitted, one at a time, to confirm the low or absent background signal from PLA probes.

Supplemental Methods

Methods for mouse genotyping, dosing doxycycline by intraperitoneal injection, thoracic duct imaging by the lipophilic fluorophore DiI, measuring wet-to-dry lung weight ratios, and performing immunohistochemistry, morphometric measurements of lymphatics, cell counting by FACS, real-time RT-PCR, and western blots are described in Supplemental Methods.

Statistical analysis

Data are presented as means ± standard error of the mean (SEM) with 8 to 10 mice per group unless otherwise indicated. Differences were assessed by analysis of variance (ANOVA) followed by Dunn-Bonferroni's test for multiple comparisons. P values < 0.05 were considered statistically significant.

RESULTS

Tracheal lymphangiectasia

VEGF-C expression was activated in the respiratory tract of double transgenic CCSP-rtTA/tetO-VEGF-C mice at ages ranging from late gestation to adult by administration of doxycycline. In these mice, doxycycline activates (Tet-On) VEGF-C expression in respiratory epithelial cells under control of the CCSP promoter (see Supplemental Methods). VEGF-C expression was intended to expand the network of lymphatics in the airways and lung. Doxycycline in drinking water was given to pregnant mice with embryos from E15.5 to E18.5, to maternal mice with pups from age P0 to P21, or to CCSP-VEGF-C mice from age P21 to P70. Embryos younger than E15.5 were not studied because strong expression of VEGFR-3 in vascular endothelial cells can result in VEGF-C-mediated changes in blood vessels as well as in lymphatics [19]. In the absence of doxycycline, double-transgenic mice had no apparent abnormalities at any of these ages.

All pups that received doxycycline in utero beginning on E15.5 (N = 26) were found dead soon after birth. All had pleural effusion at autopsy. When doxycycline was started on E16.5 (N = 33), 70% of newborn pups were found dead, and the remaining 30% had respiratory distress, cyanosis (Figure 1A), pleural effusion (Figure 1B), and died within a few hours. In contrast to the distinctive segmented lymphatic network of the normal trachea (Figure 1C), lymphatics, marked by LYVE-1 staining, were merged into sheets that formed the walls of irregularly shaped, flattened sacs throughout much of the mucosa (Figure 1D). When doxycycline was started at P0 (N = 40), 20% of pups had chylothorax at P14 (Figure 1E) but most survived.

The distribution of lymphatics examined in tracheal cross-sections from CCSP-VEGF-C mice was strikingly different in pups on water from those on doxycycline from P0 to P14 (Figure 1F, G). In the controls, lymphatics were scattered around the tracheal circumference, mainly between cartilage rings (Figure 1F, H), but in mice on doxycycline, sheets of lymphatic endothelial cells were located beneath the epithelium of almost the entire trachea (Figure 1G, I). To determine whether the sheets of lymphatic endothelial cells had a lumen, we evaluated cell polarity by determining the distribution of the luminal surface marker podocalyxin [38]. The results clearly showed that podocalyxin was restricted to the surface of the lymphatic endothelium that bordered a lumen, unlike LYVE-1 which was on both surfaces (Figure 1J, K). Lymphatic endothelial cells in mice on doxycycline had the same polarity as the controls (Figure 1J, K). Together, these findings indicate that tracheal manifestations of lymphangiectasia in CCSP-VEGF-C mice were dominated by flattened sacs that had a thin lumen and were located beneath the epithelium of the entire trachea.

Pulmonary lymphangiectasia: CCSP-VEGF-C mice vs. humans

Histological sections of lungs from CCSP-VEGF-C mice on doxycycline from P0-P14 were compared to lung sections from three children with pulmonary lymphangiectasia. Case A was a 1-month old girl who died from respiratory failure during an apparent pulmonary hypertensive crisis due to pulmonary vein stenosis. Examination of H&E-stained sections revealed widely dilated lymphatics around bronchi and large vessels and beneath the pleura (Figure 2A). Lymphatics were also enlarged in interlobular septa. The identity of the abnormal lymphatics was confirmed by D2-40/podoplanin immunoreactivity of the endothelial lining (Figure 2B-C). Enlarged lymphatics had a similar distribution in the lungs of an 11-year-old girl with pulmonary hypertension accompanied by later onset pulmonary lymphangiectasia (Case B, Supplemental Figure I A-C) and a 6-month-old boy with pulmonary lymphangiectasia associated with Down syndrome (Case C, Supplemental Figure

I D-F). The widely dilated appearance of lung lymphatics was similar in both cases, despite the difference in onset.

In H&E-stained sections of normal mouse lung, major bronchi and pulmonary blood vessels were surrounded by thin sleeves of loose connective tissue (Figure 2D). By comparison, major bronchi and vessels in lungs of CCSP-VEGF-C mice on doxycycline from P0-P14 were surrounded by prominent wide spaces (Figure 2E-F). Lymphatics stained for VEGFR-3 and Prox1 immunoreactivity were sparse around bronchi and major vessels in lungs of normal mice (Figure 2G), but were widespread in these regions of mice on doxycycline from P0 to P14 (Figure 2H). Few lymphatics were visible in regions around alveoli in either group. Unlike human lungs, mouse lungs do not have lobules or interlobular septa [39], and CCSP-VEGF-C mice did not have enlarged lymphatics in interlobular septa.

Although few or no lymphatics were found in the visceral pleura of normal mice (Figure 2I, K) [40], large flattened sacs lined by lymphatic endothelial cells were a conspicuous feature of the lung-visceral pleura interface of CCSP-VEGF-C mice on doxycycline (Figure 2J, L). To determine whether pleural mesothelial cells were actually part of the wall of these subpleural sacs, we compared the distributions of mesothelial cells identified by mesothelin immunoreactivity and lymphatic endothelial cells marked by LYVE-1 and Prox1 (Figure 2K, L). The layer of pleural mesothelial cells was distinct from Prox1-positive lymphatic endothelial cells that lined subpleural lymphatics (Figure 2L). Pleural mesothelium and lymphatic endothelium were two separate but adjacent layers.

The long-term consequences of VEGF-C overexpression were examined in lungs of CCSP-VEGF-C mice that received doxycycline for 14 weeks from P0 to P98 (Supplemental Figure II). Large lymphatic spaces, similar to and not more extensive than those found after doxycycline from P0 to P14, were located around major bronchi and lung vessels and beneath the visceral pleura. No leukocyte influx was evident in H&E-stained sections of lung. Bronchial lymph nodes, the sentinel nodes for the airways and lung, were normal in size and similar to corresponding lymph nodes in single transgenic littermates.

Fluid accumulation in lungs with lymphangiectasia

Mice with severe pulmonary lymphangiectasia had edematous lungs as well as pleural effusions. Wild-type and single transgenic mice treated with doxycycline for 5 weeks had essentially the same average values for wet weight, dry weight, and wet/dry ratio (Figure 2M). By comparison, all of these values were significantly greater in CCSP-VEGF-C mice on doxycycline (Figure 2M). The 10% increase in wet/dry ratio reflected the significant accumulation of fluid in lungs of mice that survived for 5 weeks with pulmonary lymphangiectasia. The 25% increase in lung dry weight, without evidence of inflammatory cell influx in H&E-stained sections (data not shown), was consistent with solute accumulation and lung remodeling in the presence of lymphangiectasia.

The presence of lung edema indicated a disturbance of the balance between fluid leakage and clearance. In addition to the structural abnormalities of lymphangiectatic vessels, the lymphatic endothelial cells lacked discontinuous, button-like intercellular junctions normally found in initial lymphatics (Figure 3A, C). These junctions are thought to be necessary for efficient cell and fluid entry [27, 28]. Instead, the cells were joined by continuous junctions (Figure 3B, D), similar to those present in normal collecting lymphatics and in initial lymphatics at sites of inflammation [27, 28].

Abnormalities in thoracic duct and other organs

The presence of pleural effusion at birth in CCSP-VEGF-C embryos on doxycycline from E16.5 was a sign of lymphatic dysfunction in utero. We asked whether defects in the

thoracic duct contributed to pleural effusion or chylothorax. The thoracic duct of normal newborn Prox1-GFP mice on doxycycline from E16.5 was filled with chyle after nursing (Figure 3E, left), but the thoracic duct of newborn CCSP-VEGF-C mice lacked chyle and was almost invisible (Figure 3E, right). To learn why chyle was not present, the structure of the thoracic duct was examined in situ in Prox1-GFP mice. The thoracic duct in normal mice had a tubular shape with valves at regular intervals (Figure 3F, left), but the thoracic duct of Prox1-GFP/CCSP-VEGF-C triple transgenic mice on doxycycline had aneurismal bulges and irregularly spaced valves (Figure 3F, right). To test the barrier function of thoracic duct wall, the lipophilic fluorophore DiI was administrated in milk given orally by pipette. The thoracic duct of normal neonates was sharply defined by red fluorescence at 2 hours (Figure 3G, left), but the red tracer leaked out in CCSP-VEGF-C neonates (Figure 3G, right) and accumulated in pleural fluid.

To determine whether VEGF-C overexpression in respiratory epithelial cells had effects outside the thorax, we surveyed the lymphatics of other organs. Lymphatics on the pleural surface of the diaphragm had a tubular shape in controls but were irregular sheets and sacs in CCSP-VEGF-C mice on doxycycline (Supplemental Figure III A). However, no evidence of lymphangiectasia was found outside the chest. Lymphatics in the skin and mesentery of mice on doxycycline were similar to those in controls (Supplemental Figure III B, C).

Critical period of lymphatic sensitivity to VEGF-C

VEGF-C overexpression in late gestation or during the neonatal period had more severe consequences than in older mice. Lymphangiectasia was found only after VEGF-C overexpression occurred in young mice. To define the age range during which VEGF-C overexpression resulted in pulmonary lymphangiectasia, we compared the effects of beginning doxycycline at increasing ages ranging from E15.5 to P70. The differences were striking. Lymphangiectasia became less severe with increasing age and was not found after age P35.

The most severe pulmonary lymphangiectasia was found in pups exposed to doxycycline starting at E15.5. All of these mice died before or at birth. When doxycycline was started at E16.5, 30% of the pups survived beyond P0, and lymphangiectasia was widespread in the lungs at P1. Lymphatics marked by VEGFR-3 immunoreactivity occupied 52% of lung sectional area instead of the normal 3% (Figure 4A, B). Lungs of mice on doxycycline from P0 to P7 had extensive lymphangiectasia, including subpleural lymphatics (VEGFR-3 staining, 21%, Figure 4C), but less than when started at E16.5. Mice on doxycycline for 7 days beginning at ages ranging from P14 to P35 developed mild-to-moderate pulmonary lymphangiectasia, but chylothorax did not occur and survival was not compromised (data not shown).

After age P35, doxycycline administration was accompanied by lymphatic sprouting with little or no lymphangiectasia. Lungs had few or no subpleural lymphatics. Adult mice on doxycycline from P70 to P77 had double the normal abundance of lung lymphatics (VEGFR-3 staining, 6%, Figure 4D), but the lymphatics were more normal in structure, and pleural effusion or chylothorax did not develop.

Changes in the lymphatic vasculature of the trachea provided additional insights into the age-related differences in sensitivity to VEGF-C overexpression. Tracheal lymphatics in normal neonates at P7 resembled the simple, segmental pattern of the adult (Figure 4E). Most lymphatics were located between cartilage rings; regions over cartilage rings and the trachealis muscle had few or none. When doxycycline was given from P0 to P7, what appeared to be sheets of lymphatic endothelial cells were throughout the tracheal mucosa (Figure 4F). The sheets were actually flattened bags with a narrow lumen located beneath

the epithelium (Figure 1G, I, K). Subepithelial mucosal lymphatics were located over cartilages, between cartilages, and over the trachealis muscle (Figure 4F).

In adult CCSP-VEGF-C mice on doxycycline from P70 to P77, lymphatic sprouts grew in the mucosa overlying cartilage rings (Figure 4G, H) but not over the trachealis muscle. Lymphatic growth was greater caudally than rostrally, which is consistent with previous reports of the distribution of Clara cells in the tracheobronchial epithelium of mice [41].

PECAM-1 immunoreactivity of lymphatic endothelial cells resulted in stronger staining in the tracheal mucosa of neonatal and adult CCSP-VEGF-C mice on doxycycline, but changes in tracheal blood vessels were not evident (Figure 4I-L).

At baseline, the overall abundance of tracheal lymphatics was similar at ages P7 and P77 (area density, 33% vs. 34%, Figure 4M). The value increased to 96% in neonates but only to 55% in adults on doxycycline for 7 days (Figure 4M). Lymphatics over cartilage rings, which reflected sprouting, were similarly sparse at baseline at P7 and P77 (area density, 6% vs. 9%), but the value was 100% in neonates on doxycycline, where the entire region over cartilage rings was covered by lymphatic endothelial cells (Figure 4N). The value was 66% in adult mice on doxycycline (Figure 4N). Blood vessels in the region did not change under these conditions (Figure 4O).

Mechanism of pulmonary lymphangiectasia in neonates

To explore possible mechanisms underlying the exaggerated response in neonatal CCSP-VEGF-C mice that led to lymphangiectasia, we compared the expression of VEGF-C and CCSP and the regulation of VEGF receptor signaling using changes in the trachea as readouts.

VEGF-C and rtTA mRNA—We first asked whether VEGF-C expression was greater in neonates than in adults. Measurements by qRT-PCR of VEGF-C mRNA in the trachea revealed values in neonates on doxycycline from P0 to P7 averaging 55 times those of controls without doxycycline, but the values for adults on doxycycline from age P70 to P77 were only twice the control (Figure 5A). The much larger increase in neonates resulted from smaller baseline values and larger post-doxycycline values. We next asked whether this large difference between neonates and adults was simply explained by a difference in CCSP promoter activity and thus resulted from a peculiarity of the transgene construct rather than relevant underlying biology. This proved not to be the case, as rtTA expression was greater in adults than in neonates, both at baseline and after doxycycline (Figure 5B). Because the differences in rtTA expression were in the opposite direction to VEGF-C expression, they seemed unlikely to explain the development of lymphangiectasia in neonates. This led us to determine whether the amount or distribution of the cellular source of VEGF-C differed in neonates and adults.

Amount and distribution of VEGF-C immunoreactivity—Consistent with differences in expression assessed by qRT-PCR, VEGF-C immunoreactive epithelial cells had stronger staining and were more abundant in mice on doxycycline than on water (Figure 5C) and in neonates than in adults (Figure 5D, E). VEGF-C colocalized with CCSP-immunoreactive cytoplasmic granules in Clara cells (Figure 5D, E lower). Despite this difference in amount, the distribution of VEGF-C-positive cells was about the same in neonates and adults. At both ages, VEGF-C cells were more numerous between tracheal cartilage rings than over the rings, consistent with the known distribution of CCSP-expressing Clara cells [26]. VEGF-C immunoreactivity was similarly faint or absent in the tracheal epithelium of neonates and adults in the absence of doxycycline (Figure 5F, G).

Similar results were obtained with two different VEGF-C antibodies (see Supplemental Methods).

Doxycycline-VEGF-C expression dose-response—To test whether the difference in VEGF-C expression was indeed responsible for lymphangiectasia developing in neonates but not in adults, we matched the VEGF-C expression at the two ages by taking advantage of doxycycline regulation of VEGF-C transgene expression through the Tet-on system [42]. The goal was to learn whether lymphangiectasia still developed in neonates when VEGF-C production was reduced to the adult level by lowering doxycycline intake.

We found that expression of VEGF-C mRNA in neonates increased in a log-linear manner with doxycycline concentration over the range of 0 to 5 mg/ml (Figure 5H). Baseline VEGF-C expression was essentially the same as in wild-type mice, indicating minimal leakage of transgene expression without doxycycline (Figure 5H). VEGF-C expression and lymphangiectasia increased progressively at doxycycline concentrations above 0.01 mg/ml. The dose-response relationship enabled us to identify the doxycycline concentration (0.1 mg/ml) that produced in neonates the same low level of VEGF-C mRNA expression as found in adults. Importantly, at that concentration, lymphangiectasia developed in neonates but not in adults, even though the VEGF-C expression was matched (Figure 5I). The number and distribution of VEGF-C positive epithelial cells were similar at both ages under this condition (Supplemental Figure IV). Neonates developed moderate lymphangiectasia at an even lower doxycycline concentration (0.01 mg/ml), but adults had only lymphatic sprouting (Figure 5J).

Chylothorax developed only when the pups received the highest concentration of doxycycline (5 mg/ml). Mice receiving doxycycline at 0.1 mg/ml from E16.5 had 35% mortality by P0, compared to 70% for those receiving 5 mg/ml, but all died by P4 (N = 14). Pups on doxycycline at 1 mg/ml from P0 to P14 did not develop chylothorax (N = 30).

Matching doxycycline intake in neonates and adults—Because neonates received doxycycline via the mother by drinking milk and adults received it by drinking water, we asked whether this difference could explain the greater expression of VEGF-C in neonates. To address the issue, we estimated the dose of doxycycline received by neonates via milk (see Supplemental Methods) and gave this dose (100 μg/g) to newborns and adults by intraperitoneal (ip) injection to circumvent the oral route altogether. Neonates – but not adults - developed lymphangiectasia, and the severity resembled that found with oral doxycycline at a concentration of 5 mg/ml (data not shown).

Proteolytic cleavage forms of VEGF-C—As another possible factor contributing to the age-dependency of lymphangiectasia in CCSP-VEGF-C mice, we asked whether proteolytic processing of VEGF-C differed in neonates and adults. Proteolytic processing of VEGF-C from the native to mature form increases receptor binding affinity [21], which could contribute to lymphangiogenic potency. In western blots, the band for VEGF-C protein was similarly weak in tracheas of neonates and adults under baseline conditions (Figure 5K). Compared to the baseline value, after doxycycline for 7 days, intermediate forms of VEGF-C were 10 times as abundant in neonates and only twice as abundant in adults. Yet, the mature form of VEGF-C was still faint in neonates but was readily visible in adults. Native full-length VEGF-C (58 kDa) was not detected in tracheas of mice on doxycycline at either age, but the high background from the probing antibody at the expected molecular weight limited detection of weak signals.

Together, these experiments examine multiple factors that could contribute to the age-dependency of lymphangiectasia in CCSP-VEGF-C mice. Although neonates had higher

expression of VEGF-C than adults, this difference did not explain the development of lymphangiectasia because neonates still developed lymphangiectasia when VEGF-C expression matched that in the adult. Age-related differences in CCSP promoter activity, Clara cell distribution, or efficiency of doxycycline delivery were also excluded. Age-related differences in proteolytic processing or receptor signaling could, however, contribute.

VEGFR-2 and VEGFR-3 signaling in pulmonary lymphangiectasia

Comparison of the distribution of VEGFR-2 and VEGFR-3, the receptors for VEGF-C, revealed immunoreactivity for both receptors on lymphatics in the tracheas of neonatal and adult CCSP-VEGF-C mice under baseline conditions. VEGFR-3 immunoreactivity was mainly on lymphatics. Staining for VEGFR-2 was stronger on blood vessels than lymphatics (Figure 6A, C). The intensity of staining for the receptors did not change noticeably after doxycycline for 7 days, but both were much more widespread because of the expansion of lymphatic endothelial cells, which was much greater in neonates than adults (Figure 6B, D).

Measurements of VEGFR-2 and VEGFR-3 mRNA by qRT-PCR revealed higher expression in the trachea of mice on doxycycline for 7 days and greater expression in neonates than in adults (Figure 6E). VEGFR-3 expression was increased much more than VEGFR-2, although the apparent change in VEGFR-2 was confounded by high baseline expression of VEGFR-2 in blood vessels. The increase in VEGFR-3 was much larger in neonates (7.4-fold) than in adults (2-fold). VEGFR-2 and VEGFR-3 protein assessed by western blot was also greater in neonates than in adults (Figure 6F).

VEGFR-2 and VEGFR-3 are expressed on some inflammatory cells [43, 44]. To determine whether activation of VEGF-C expression in the airway and lung epithelium leads to inflammatory cell recruitment, we used the pan-leukocyte marker CD45 and selective leukocyte markers (Iba1 for macrophages, S100A9 for neutrophils, B220 for B cells, and CD3e for T cells) to determine the magnitude and type of inflammatory cell influx into the tracheas and lungs of neonates by immunohistochemical staining and qRT-PCR analysis. Cells with CD45 or Iba1 immunoreactivity were sparse in the tracheal mucosa of control mice and in CCSP-VEGF-C mice on doxycycline (Supplemental Figure V A-B). Similarly, few cells with S100A9, B220, or CD3e immunoreactivity were found in control or doxycycline-treated tracheas (Supplemental Figure V C-E). Double staining for VEGFR-3 and each of the five leukocyte markers showed no apparent association under any of the conditions (Supplemental Figure V A-E). The mRNA levels measured for these five markers revealed no significant differences in the trachea and lungs between controls and doxycycline-treated mice (Supplemental Figure V F).

We next asked whether the increase in VEGFR-2 and VEGFR-3 expression could be explained by the greater number of lymphatic endothelial cells or whether greater receptor expression per cell made a significant contribution. We estimated the number of lymphatic endothelial cells in the trachea in three ways. First, the number of lymphatic endothelial cells in the tracheas was estimated by FACS using lymphatic endothelial cell markers after tissue digestion (see Supplemental Methods). An average of only 35 lymphatic endothelial cells were obtained per trachea from neonates (Supplemental Figure VI). Even in the trachea of adults, the number was small (120 cells per trachea), yet as a control for the methods, the number obtained from adult ears was much greater (1920 cells per mouse). Because of the poor yield from tracheas in the FACS approach, the low values were considered unreliable. Second, Prox1-positive nuclei were counted, and the number was scaled to the overall area of LYVE-1 immunoreactivity (see Supplemental Methods). Based on this method, the number of lymphatic endothelial cells increased 6.5-fold in mice on doxycycline from P0 to P7, from 13,787 cells to 89,057 cells. Third, comparison of Prox1 mRNA expression in the trachea of P7 mice on doxycycline to corresponding baseline controls gave a 7-fold increase.

According to the second and third approaches, roughly 90% of the increase in VEGFR-3 could be attributed to lymphatic endothelial cell proliferation in the trachea of neonates on doxycycline.

The relative contribution of VEGFR-2 and VEGFR-3 signaling to the development of lymphangiectasia was tested by treating newborn mice from P0 to P7 on doxycycline concurrently with function blocking antibodies to VEGFR-2 (DC101), VEGFR-3 (mF4-31C1), or both (Figure 6G). Inhibition of VEGFR-2 alone had little effect on lymphangiectasia and reduced tracheal lymphatics by only 14% compared to age-matched controls (Figure 6H), but did result in regression of some tracheal blood vessels (data not shown), as reported previously [45]. Inhibition of VEGFR-3 alone reduced lymphatics by 40%. However, when VEGFR-2 and VEGFR-3 were blocked together, the amount of lymphangiectasia was reduced 90%, which was much larger than the sum of effects of blocking the individual receptors (54% reduction), consistent with synergistic actions of the receptors (Figure 6H).

Lymphatic sprouts over cartilage rings were measured as another readout of lymphangiogenesis in neonates on doxycycline. Lymphatic sprouts were reduced 5% by blocking VEGFR-2, were reduced 21% by blocking VEGFR-3, but were reduced 91% by blocking both receptors together (Figure 6I). The much larger effect of VEGFR-2 and VEGFR-3 blockade together, in comparison to the sum of effects of blocking individual receptors (26% reduction), was additional evidence of synergistic actions of the receptors.

The link of receptor synergy to lymphangiectasia was further explored by performing similar experiments on adult mice treated with blocking antibodies during doxycycline administration from P70 to P77 (Figure 6J, K). These experiments showed that lymphatic sprouts over cartilage rings were reduced 33% by blocking VEGFR-2 but were reduced 94% by blocking VEGFR-3. Inhibition of both receptors together resulted in 99% reduction in lymphatic sprouts, indicating that concurrent inhibition of VEGFR-2 added little to the already large effect of VEGFR-3 blockade. The minimal increment of blocking VEGFR-2 concurrently fits with the dominance of VEGFR-3 signaling in adult lymphangiogenesis and contrasts with the synergistic actions of the two receptors in neonates.

VEGFR-2/VEGFR-3 heterodimers in pulmonary lymphangiectasia

To explore the apparent synergistic actions of VEGFR-2 and VEGFR-3 in mediating the development of pulmonary lymphangiectasia, we asked whether the exaggerated signaling in neonates involved the formation of receptor heterodimers. Using in situ proximity ligation assay (PLA) [37] to detect VEGFR-2/VEGFR-3 heterodimers, we compared PLA dots (heterodimer signals) in lymphatic endothelial cells in the trachea of neonates and adults on water or doxycycline for 7 days. PLA dots were associated with lymphatic endothelial cells in all groups but were most abundant in neonates on doxycycline (Figure 7A-D). Confirmation that PLA dots were associated with lymphatics was obtained by using LYVE-1 to mark lymphatic endothelial cells and DAPI to mark nuclei (Figure 7E). Measurements revealed that PLA dots per lymphatic endothelial cell nucleus were twice as abundant in neonates under baseline conditions and 4 times as abundant in neonates on doxycycline, compared to corresponding values in adults (Figure 7F).

Reversibility of pulmonary lymphangiectasia

Because of the reversibility of doxycycline-induced activation of the CCSP-rtTA driver [34], we asked whether lymphangiectasia resolved after withdrawal of doxycycline. Newborn CCSP-VEGF-C mice were given doxycycline from P0 to P7 and then water from P7 to P14. Lymphangiectasia was still widespread at P14 (Figure 8A, B). To determine the rate of

decrease in VEGF-C expression after doxycycline withdrawal, VEGF-C mRNA was measured in tracheas after doxycycline from P0 to P7 and then water for one to 4 weeks. VEGF-C expression decreased 20% at 1 week, 55% at 2 weeks, 70% at 3 weeks, and 100% at 4 weeks (Figure 8C). This relatively slow decline could reflect the slow clearance of doxycycline [46]. Because of the slow decrease in VEGF-C after removal of doxycycline, we tested the reversibility of lymphangiectasia by function blocking antibodies to VEGFR-2 and VEGFR-3 receptors while off doxycycline from P7 to P14. Lymphangiectasia was minimally reversed by this approach (Figure 8D, E). The reduction was 1% after inhibition of VEGFR-2, 2% after inhibition of VEGFR-3, and 10% after inhibition of both receptors (Figure 8E).

To test reversibility over a longer period, lymphangiectasia was measured in mice on doxycycline from P0 to P7 and then on water for 19 months. Lymphangiectasia was still strikingly widespread in the trachea (Figure 8F). Measurements showed that the amount of lymphangiectasia was reduced only 24% (Figure 8E), and the overall appearance of the sheets of lymphatic endothelial cells was still highly abnormal and resembled that found after inhibition of VEGFR-2 and VEGFR-3 together for a week (Figure 8D).

DISCUSSION

This study of CCSP-VEGF-C double transgenic mice revealed unexpectedly that a condition resembling pulmonary lymphangiectasia developed when VEGF-C was overexpressed in the respiratory epithelium of neonates. Affected mice had respiratory distress, cyanosis, pleural effusion, chylothorax, and high mortality. Like pulmonary lymphangiectasia in humans, the condition in CCSP-VEGF-C mice was characterized by abundant large sac-like lymphatics around major bronchi and pulmonary blood vessels and beneath the pleura. Lymphangiectasia was most severe when VEGF-C was overexpressed between the ages of E15.5 and P14 and was minimal or absent in mice older than P35. Mechanistic studies revealed that lymphangiectasia resulted from exaggerated responses of lymphatics of neonates to VEGF-C. Signaling of both VEGFR-3 and VEGFR-2 was required for development of lymphangiectasia in neonates, unlike lymphangiogenesis in the adult where VEGFR-3 signaling was sufficient. The involvement of both receptors in lymphangiectasia was supported by the presence of heterodimers of VEGFR-2 and VEGFR-3 in lymphatics in neonates. Once formed, lymphangiectasia resisted regression after withdrawal of VEGF-C or inhibition of its receptors.

Comparison of lymphangiectasia in CCSP-VEGF-C mice and humans

CCSP-VEGF-C mice were created to determine whether the magnitude or duration of inflammatory responses in the airways could be reduced by expanding the lymphatic network to increase fluid and cell clearance. Instead, overexpression of VEGF-C in respiratory epithelial cells unexpectedly led to the growth of widely dilated lymphatics in the form of irregular sacs around major bronchi and pulmonary vessels and beneath the visceral pleura. In so doing, the model serendipitously offered the opportunity to examine the development of pulmonary lymphangiectasia. The changes in CCSP-VEGF-C mice were similar to the pathology found in pulmonary lymphangiectasia in humans, as reflected by three cases shown herein and many other published cases [4-6]. This similarity raises the possibility of mechanistic parallels that could help in understanding how lymphangiectasia develops in humans, albeit VEGF-C overexpression in the respiratory epithelium is unlikely to contribute to the etiology in humans as it does in CCSP-VEGF-C mice.

Chylothorax is among other abnormalities found in both CCSP-VEGF-C mice and in pulmonary lymphangiectasia in humans. Chylothorax in CCSP-VEGF-C mice was a manifestation of early onset and severe lymphatic dysfunction and could have resulted from

thoracic duct defects due to high levels of VEGF-C in the pleural fluid, but this is yet to be demonstrated. If this is true, VEGF-C could serve as a biomarker relevant to survival and prognosis. Fluid accumulation in the lungs also occurs in both settings. In CCSP-VEGF-C mice, this was reflected by increased total lung water and wet to dry weight ratio and was accompanied by edema around major bronchi and pulmonary vessels.

Lymphatic malformations in the lung are typically in the form of a generalized lymphatic anomaly, also known as diffuse lymphangiomatosis, which overlaps clinically and histologically with pulmonary lymphangiectasia [16]. Lymphatic malformations, previously termed lymphangiomas, are a source of serious morbidity in children. They most commonly involve soft tissues in the neck, axillae, groin/perineum, chest wall, tongue, and proximal limbs and occasionally affect viscera [15]. They are generally non-familial and idiopathic, but an understanding of their etiologies is gradually unfolding as genetic underpinnings are identified in a subset of patients [13].

As the search for the underlying cause of lymphangiectasia continues, recent studies of transgenic mouse embryos have implicated gain-of-function mutations in the RAS signaling pathway, including RAF1, during development of lymphatic endothelial cells [47]. Furthermore, mice lacking phosphatidylinositol 3-kinase, regulatory subunit 1 (PIK3R1) develop intestinal lymphangiectasia and chylous ascites at birth, but no changes were reported in lungs [48]. It is expected that insights into the pathobiology of pulmonary lymphangiectasia will not only lead to insights into the treatment of patients with this disease, including severe forms which are increasingly survivable in the modern era of neonatal intensive care [9, 49], but will also improve the understanding of the physiology and treatment of other lymphatic anomalies.

Lymphangiectasia and lung inflammation

Although bacterial pneumonia is well known to complicate chronic lung disease of all sorts, including pulmonary lymphangiectasia [50, 51], inflammation is not a part of the classic description or classification scheme for developmental lymphatic disorders of the human thorax [52] and is not required for diagnosis. Intraluminal lymphocytes as a component of lymph fluid can be found in lymphangiectasia [53], and malformed intrapulmonary lymphatic channels [8] can be focally lined by lymphoid aggregates, but neither is considered inflammation. Similarly, macrophages can be more abundant in alveolar spaces next to lymphatic malformations [8, 54] but generally do not infiltrate the tissue as in sites of inflammation.

Because some inflammatory cells express VEGF-C or support VEGFR-2 and/or VEGFR-3 signaling, which could contribute to the development of lymphangiectasia, we determined whether inflammatory cells were recruited to the trachea or lungs of CCSP-VEGF-C mice. No such influx was found by histologic examination, immunohistochemical staining, or qRT-PCR. These findings indicate little or no role of inflammatory cells in promotion of lymphangiectasia in this model and show that VEGF-C overexpression can promote lymphangiectasia in the absence of inflammatory cell recruitment.

Critical period of lymphatic hypersensitivity to VEGF-C

The response of lymphatics to doxycycline regulated VEGF-C overexpression was strikingly different in neonates and adults. Lymphangiectasia developed in neonatal CCSP-VEGF-C mice over a 5000-fold range of doxycycline concentration (10^{-3} to 5 mg/ml), but did not occur in adults at even the highest concentration. Similarly, lymphangiectasia developed in neonates but not adults even when the number and distribution of VEGF-C producing cells were matched by customizing the doxycycline administration. These

findings suggest that lymphatics in neonates are more prone to abnormal growth in response to VEGF-C.

Lymphatics in the lungs of neonatal CCSP-VEGF-C mice were abundant in lung parenchyma and beneath the visceral pleura, where they were normally sparse or absent. The vessels from which the subpleural lymphatics grew in these mice was not determined, but lymphatics in the adjacent parenchyma were a likely possibility. Lymphatics in fibrotic lung disease have been suggested to form from CD11b-positive alveolar macrophages [55]. Yet, lymphangiogenesis in adult lungs tends to occur preferentially in regions around major bronchi and blood vessels, similar to where they grow near lung tumors that overexpress VEGF-C [56].

It is unclear whether the type of response found in the airways and lung of CCSP-VEGF-C mice can occur elsewhere. Lymphangiectasia was not reported in studies of VEGF-C overexpression in skin of K14-rtTA/tetO-VEGF-C mice [19], but the timing of doxycycline and methods of analysis differed from the present study. Testing the effects of VEGF-C driven by other tissue-specific promoters should expand the understanding of age-dependent differences in sensitivity of lymphatic endothelial cells to VEGF-C.

Greater VEGF-C expression in neonatal CCSP-VEGF-C mice

An important step in assessing the basis of greater VEGF-C production in neonatal CCSP-VEGF-C mice was to ask whether the response to doxycycline of the CCSP-rtTA driver was age-dependent. Fortunately, CCSP-rtTA driver mice have been used to control gene expression in the lung of multiple transgenic models, and multiple driver lines have been developed [33, 36, 57]. Neonates in one of the CCSP-rtTA driver lines were found to have greater expression than adults [58], but our measurements of rtTA mRNA expression in the trachea of CCSP-rtTA mice showed lower values in neonates. Consistent with this finding, no significant difference was found between neonatal and adult CCSP-rtTA-driven expression of luciferase or IL-1beta in mice derived from the same driver mice used in present study [34, 36]. These findings indicate that an age-dependent difference in CCSP-rtTA expression was not essential for greater VEGF-C expression in neonates.

Although low concentrations of doxycycline led to the development of pulmonary lymphangiectasia in neonatal CCSP-VEGF-C mice, larger amounts were necessary for the development of chylothorax and changes accompanied by high mortality. Future studies are needed to elucidate factors that underlie these differences.

Incomplete VEGF-C processing in neonatal mice with pulmonary lymphangiectasia

Native full-length 58 kDa VEGF-C undergoes proteolytic processing to generate the mature form, which has greater binding affinity for VEGFR-2 and VEGFR-3 [21]. The extent of proteolytic processing of VEGF-C is determined by multiple factors, and the amount of the shorter forms influences activity [59]. We found that most of the VEGF-C in neonatal CCSP-VEGF-C mice was not the fully processed mature 20 kDa form, suggesting a limiting step in VEGF-C protein cleavage during this critical period of development. The tracheas of neonates had much more partially processed VEGF-C than adults. Although the difference was striking, the contribution to the abnormal response of lymphatics remains to be determined. Proteolytic processing is also required for activation of VEGF-D [60], and partially processed VEGF-D can induce VEGFR-2/VEGFR-3 heterodimerization [61]. It is unknown whether partially processed VEGF-C has this property.

The binding affinity of VEGF-A isoforms for heparan sulfate proteoglycans influences angiogenic activity [62]. Less is known of this property of VEGF-C, which does not have a conventional heparin-binding domain in the primary protein sequence. However, interaction

with heparin can influence the pattern of VEGF-C-induced lymphangiogenesis [63]. Fully processed VEGF-C can bind heparan sulfate [64], but the extent of binding of longer forms of VEGF-C has not been determined. Further work is needed to understand the links between proteolytic processing of VEGF-C, binding to extracellular matrix, and development of lymphangiectasia.

Involvement of VEGFR-2, VEGFR-3, and heterodimers in lymphangiectasia

Based on effects of selective blocking antibodies, VEGFR-3 signaling was sufficient to drive lymphangiogenesis in adult CCSP-VEGF-C mice, and VEGFR-2 signaling had a minor role. A similar mechanism has been found in other models of lymphangiogenesis [20, 65]. Unexpectedly, VEGFR-2 was more important in neonatal mice, as both VEGFR-2 and VEGFR-3 had to be blocked to prevent the development of lymphangiectasia. Inhibition of both receptors had a much larger effect on lymphangiectasia than the sum of the effects of blocking each receptor separately. The more-than-additive effect of blocking VEGFR-2 and VEGFR-3 together suggests that VEGF-C is not just simply saturating VEGFR-3 and then activating VEGFR-2. This raised the question of involvement of VEGFR-2/VEGFR-3 heterodimers in the synergistic actions of the receptors. The finding by proximity ligation assay of more abundant VEGFR-2/VEGFR-3 heterodimers in lymphatics of neonates than adults is consistent with this involvement.

VEGF-C can induce the formation of VEGFR-2/VEGFR-3 heterodimers in lymphatic endothelial cells [66]. Importantly, VEGFR-3 is phosphorylated at fewer tyrosine residues in VEGFR-2/VEGFR-3 heterodimers: tyrosines Tyr-1337 and Tyr-1363 are not phosphorylated in heterodimers as they are in VEGFR-3 homodimers [66]. This difference could have profound effects on signal transduction. Further experiments are needed to determine the extent heterodimers contribute to the hypersensitivity of lymphatic endothelial cells to VEGF-C during the critical period.

The function-blocking antibodies used in the present studies were generated against the ligand-binding domains of VEGFR-2 and VEGFR-3 respectively. Human versions of such antibodies are currently in clinical trails as cancer therapeutics [67]. Activation of VEGF receptors by ligand binding involves receptor dimerization [68]. A new class of blocking antibody against human VEGFR-3 had been made to inhibit the formation of VEGFR-3 homodimers and VEGFR-2/VEGFR-3 heterodimers [69]. A mouse version of the anti-dimerization antibody could help elucidate the contribution of VEGFR-2/VEGFR-3 heterodimers to pulmonary lymphangiectasia.

Limited reversibility of pulmonary lymphangiectasia

The persistence of lymphangiectasia after inhibition of VEGFR-2 and VEGFR-3 or after long-term withdrawal of the doxycycline indicated a previously unappreciated stability of these abnormal lymphatics. VEGFR-2/VEGFR-3 signaling was evidently not required for maintenance of lymphangiectasia in this model. Persistence of newly formed lymphatics in mouse airways has been reported after resolution of airway inflammation [20, 70] or withdrawal of IL-1beta in doxycycline-regulated CCSP-IL-1beta transgenic mice [26]. Similarly, new lymphatics in skin persist for many months after withdrawal of VEGF-C overexpression in transgenic mice [19]. The limited regression of lymphangiectasia is in sharp contrast to the rapid regression of blood vessels in CCSP-rtTA/tetO-VEGF-A transgenic mice after withdrawal of doxycycline [32].

Until a strategy is found to promote regression of lymphangiectatic vessels, another approach would be to improve lymphatic function by advancing maturation or “normalization” of the new lymphatics. Normalization of tumor blood vessels can have

beneficial effects on drug delivery [71]. Less is known about the normalization of lymphatics, but the principle has been demonstrated in tumors where lymphatic function was improved by inhibition of TGF-beta [72] and lymphatic maturation is promoted by treatment with glucocorticoids [28].

In summary, the present study revealed unexpectedly that doxycycline-regulated overexpression of VEGF-C in the respiratory epithelium of CCSP-VEGF-C mice during a critical period of perinatal development led to a condition resembling pulmonary lymphangiectasia in human infants. Newborn pups developed respiratory distress, cyanosis, and chylothorax, and sac-like lymphatics formed in the lung around major bronchi and pulmonary vessels and beneath the visceral pleura. Formation of lymphangiectasia required VEGF-C signaling through both VEGFR-2 and VEGFR-3 and involved the formation of receptor heterodimers. Lymphangiectasia was prevented by blocking VEGFR-2 and VEGFR-3 together but was little reversed by receptor blockade or withdrawal of VEGF-C. Studies of abnormal lymphatic growth in CCSP-VEGF-C mice should help to elucidate the mechanisms of formation and persistence of pulmonary lymphangiectasia in humans and to identify new diagnostic and therapeutic approaches.

Supplementary Material

Refer to Web version on PubMed Central for supplementary material.

Acknowledgments

We thank Dr. Jeff Whitsett of Cincinnati Children's Hospital Medical Center for donating the CCSP-rtTA mouse breeders, and Dr. Marja Lohela for making the tetO-VEGF-C mice in the Alitalo Laboratory at the University of Helsinki. We also thank Drs. Barry Stripp (Duke University) and Jason Rock (UCSF) for the kind gift of antibody to CCSP, Oishee Bose for assisting with FACS analysis and Jennifer Bolen of the UCSF Mouse Pathology Core Facility for histological staining.

SOURCES OF FUNDING

This work was supported in part by funding from the Lymphatic Malformation Institute, grants HL024136 and HL59157 from National Heart, Lung, and Blood Institute of the US National Institutes of Health, and the Leducq Foundation to DMcD, and by a postdoctoral fellowship award from the Lymphatic Research Foundation to LCY.

Nonstandard Abbreviations and Acronyms

CCSP	Clara Cell Secretory Protein
rtTA	reverse tetracycline-controlled transactivator
tetO	tetracycline operator
VEGF-C	Vascular endothelial growth factor-C
VEGFR-2	Vascular endothelial growth factor receptor-2
VEGFR-3	Vascular endothelial growth factor receptor-3
VE-cadherin	Vascular endothelial-cadherin
LYVE-1	Lymphatic vessel endothelial hyaluronan receptor 1
PECAM1	Platelet endothelial cell adhesion molecule 1
PLA	Proximity ligation assay
DAPI	4',6-diamidino-2-phenylindole

REFERENCES

1. Leak LV. Lymphatic removal of fluids and particles in the mammalian lung. Environ Health Perspect. 1980; 35:55–75. [PubMed: 6157524]
2. Randolph GJ, Angeli V, Swartz MA. Dendritic-cell trafficking to lymph nodes through lymphatic vessels. Nat Rev Immunol. 2005; 5:617–628. [PubMed: 16056255]
3. El-Chemaly S, Levine SJ, Moss J. Lymphatics in lung disease. Ann N Y Acad Sci. 2008; 1131:195–202. [PubMed: 18519971]
4. Bredt H. lymphangiectasia pulmonum congenita. Virchows Arch. 1952; 321:517–530. [PubMed: 14951108]
5. Laurence KM. Congenital pulmonary cystic lymphangiectasis. J Pathol Bacteriol. 1955; 70:325–333. [PubMed: 13295907]
6. Noonan JA, Walters LR, Reeves JT. Congenital pulmonary lymphangiectasis. Am J Dis Child. 1970; 120:314–319. [PubMed: 5493829]
7. Virchow, R. Vol. 982. Frankfurt-am-Main, Meidinger Sohn & Company; 1856. Phlogose und thrombose im gefassystem; p. 456Gesammelte Abhandlungen zur Wissenschaftlichen Medicin
8. Faul JL, Berry GJ, Colby TV, Ruoss SJ, Walter MB, Rosen GD, Raffin TA. Thoracic lymphangiomas, lymphangiectasis, lymphangiomatosis, and lymphatic dysplasia syndrome. Am J Respir Crit Care Med. 2000; 161:1037–1046. [PubMed: 10712360]
9. Barker PM, Esther CR Jr. Fordham LA, Maygarden SJ, Funkhouser WK. Primary pulmonary lymphangiectasia in infancy and childhood. Eur Respir J. 2004; 24:413–419. [PubMed: 15358700]
10. Esther CR Jr. Barker PM. Pulmonary lymphangiectasia: Diagnosis and clinical course. Pediatr Pulmonol. 2004; 38:308–313. [PubMed: 15334508]
11. Bellini C, Boccardo F, Campisi C, Bonioli E. Congenital pulmonary lymphangiectasia. Orphanet J Rare Dis. 2006; 1:43. [PubMed: 17074089]
12. Finder J, Steinfeld J. Congenital pulmonary lymphangiectasia. N Engl J Med. 2004; 350:948. author reply 948. [PubMed: 14985498]
13. Boon, LM.; Vikkula, M. Molecular genetics of vascular malformations. In: Mulliken, JB.; Burrows, PE.; Fishman, SJ., editors. Mulliken & young's vascular anomalies : Hemangiomas and malformations. Oxford University Press; England: 2013. p. 327-375.
14. Tazelaar HD, Kerr D, Yousem SA, Saldana MJ, Langston C, Colby TV. Diffuse pulmonary lymphangiomatosis. Hum Pathol. 1993; 24:1313–1322. [PubMed: 8276379]
15. Hassanein AH, Mulliken JB, Fishman SJ, Quatrano NA, Zurakowski D, Greene AK. Lymphatic malformation: Risk of progression during childhood and adolescence. J Craniofac Surg. 2012; 23:149–152. [PubMed: 22337394]
16. Fishman, SJ. Truncal, visceral, and genital vascular malformations. In: Mulliken, JB.; Burrows, PE.; Fishman, SJ., editors. Mulliken & young's vascular anomalies : Hemangiomas and malformations. Oxford University Press; England: 2013. p. 966-1016.
17. Karkkainen MJ, Haiko P, Sainio K, Partanen J, Taipale J, Petrova TV, Jeltsch M, Jackson DG, Talikka M, Rauvala H, Betsholtz C, Alitalo K. Vascular endothelial growth factor c is required for sprouting of the first lymphatic vessels from embryonic veins. Nat Immunol. 2004; 5:74–80. [PubMed: 14634646]
18. Jeltsch M, Kaipainen A, Joukov V, Meng X, Lakso M, Rauvala H, Swartz M, Fukumura D, Jain RK, Alitalo K. Hyperplasia of lymphatic vessels in vegf-c transgenic mice. Science. 1997; 276:1423–1425. [PubMed: 9162011]
19. Lohela M, Helotera H, Haiko P, Dumont DJ, Alitalo K. Transgenic induction of vascular endothelial growth factor-c is strongly angiogenic in mouse embryos but leads to persistent lymphatic hyperplasia in adult tissues. Am J Pathol. 2008; 173:1891–1901. [PubMed: 18988807]
20. Baluk P, Tammela T, Ator E, Lyubynska N, Achen MG, Hicklin DJ, Jeltsch M, Petrova TV, Pytowski B, Stacker SA, Yla-Herttuala S, Jackson DG, Alitalo K, McDonald DM. Pathogenesis of persistent lymphatic vessel hyperplasia in chronic airway inflammation. J Clin Invest. 2005; 115:247–257. [PubMed: 15668734]

21. Joukov V, Sorsa T, Kumar V, Jeltsch M, Claesson-Welsh L, Cao Y, Saksela O, Kalkkinen N, Alitalo K. Proteolytic processing regulates receptor specificity and activity of vegf-c. EMBO J. 1997; 16:3898–3911. [PubMed: 9233800]
22. Hong YK, Lange-Asschenfeldt B, Velasco P, Hirakawa S, Kunstfeld R, Brown LF, Bohlen P, Senger DR, Detmar M. Vegf-a promotes tissue repair-associated lymphatic vessel formation via vegfr-2 and the alpha1beta1 and alpha2beta1 integrins. FASEB J. 2004; 18:1111–1113. [PubMed: 15132990]
23. Goldman J, Rutkowski JM, Shields JD, Pasquier MC, Cui Y, Schmokel HG, Willey S, Hicklin DJ, Pytowski B, Swartz MA. Cooperative and redundant roles of vegfr-2 and vegfr-3 signaling in adult lymphangiogenesis. FASEB J. 2007; 21:1003–1012. [PubMed: 17210781]
24. Baldwin ME, Halford MM, Roufail S, Williams RA, Hibbs ML, Grail D, Kubo H, Stacker SA, Achen MG. Vascular endothelial growth factor d is dispensable for development of the lymphatic system. Mol Cell Biol. 2005; 25:2441–2449. [PubMed: 15743836]
25. Haiko P, Makinen T, Keskitalo S, Taipale J, Karkkainen MJ, Baldwin ME, Stacker SA, Achen MG, Alitalo K. Deletion of vascular endothelial growth factor c (vegf-c) and vegf-d is not equivalent to vegf receptor 3 deletion in mouse embryos. Mol Cell Biol. 2008; 28:4843–4850. [PubMed: 18519586]
26. Baluk P, Hogmalm A, Bry M, Alitalo K, Bry K, McDonald DM. Transgenic overexpression of interleukin-1beta induces persistent lymphangiogenesis but not angiogenesis in mouse airways. Am J Pathol. 2013
27. Baluk P, Fuxe J, Hashizume H, Romano T, Lashnits E, Butz S, Vestweber D, Corada M, Molendini C, Dejana E, McDonald DM. Functionally specialized junctions between endothelial cells of lymphatic vessels. J Exp Med. 2007; 204:2349–2362. [PubMed: 17846148]
28. Yao LC, Baluk P, Srinivasan RS, Oliver G, McDonald DM. Plasticity of button-like junctions in the endothelium of airway lymphatics in development and inflammation. Am J Pathol. 2012; 180:2561–2575. [PubMed: 22538088]
29. Huggenberger R, Siddiqui SS, Brander D, Ullmann S, Zimmermann K, Antsiferova M, Werner S, Alitalo K, Detmar M. An important role of lymphatic vessel activation in limiting acute inflammation. Blood. 2011; 117:4667–4678. [PubMed: 21364190]
30. Zhou Q, Guo R, Wood R, Boyce BF, Liang Q, Wang YJ, Schwarz EM, Xing L. Vascular endothelial growth factor c attenuates joint damage in chronic inflammatory arthritis by accelerating local lymphatic drainage in mice. Arthritis Rheum. 2011; 63:2318–2328. [PubMed: 21538325]
31. Lee CG, Link H, Baluk P, Homer RJ, Chapoval S, Bhandari V, Kang MJ, Cohn L, Kim YK, McDonald DM, Elias JA. Vascular endothelial growth factor (vegf) induces remodeling and enhances th2-mediated sensitization and inflammation in the lung. Nat Med. 2004; 10:1095–1103. [PubMed: 15378055]
32. Baluk P, Lee CG, Link H, Ator E, Haskell A, Elias JA, McDonald DM. Regulated angiogenesis and vascular regression in mice overexpressing vascular endothelial growth factor in airways. Am J Pathol. 2004; 165:1071–1085. [PubMed: 15466375]
33. Tichelaar JW, Lu W, Whitsett JA. Conditional expression of fibroblast growth factor-7 in the developing and mature lung. J Biol Chem. 2000; 275:11858–11864. [PubMed: 10766812]
34. Perl AK, Tichelaar JW, Whitsett JA. Conditional gene expression in the respiratory epithelium of the mouse. Transgenic Res. 2002; 11:21–29. [PubMed: 11874100]
35. Choi I, Chung HK, Ramu S, Lee HN, Kim KE, Lee S, Yoo J, Choi D, Lee YS, Aguilar B, Hong YK. Visualization of lymphatic vessels by prox1-promoter directed gfp reporter in a bacterial artificial chromosome-based transgenic mouse. Blood. 2011; 117:362–365. [PubMed: 20962325]
36. Bry K, Whitsett JA, Lappalainen U. Il-1beta disrupts postnatal lung morphogenesis in the mouse. Am J Respir Cell Mol Biol. 2007; 36:32–42. [PubMed: 16888287]
37. Nilsson I, Bahram F, Li X, Gualandi L, Koch S, Jarvius M, Soderberg O, Anisimov A, Kholova I, Pytowski B, Baldwin M, Yla-Herttuala S, Alitalo K, Kreuger J, Claesson-Welsh L. Vegf receptor 2/-3 heterodimers detected in situ by proximity ligation on angiogenic sprouts. EMBO J. 2010; 29:1377–1388. [PubMed: 20224550]

38. Kerjaschki D, Sharkey DJ, Farquhar MG. Identification and characterization of podocalyxin--the major sialoprotein of the renal glomerular epithelial cell. J Cell Biol. 1984; 98:1591–1596. [PubMed: 6371025]
39. McLaughlin RF Jr. Tyler WS, Canada RO. Subgross pulmonary anatomy of the rabbit, rat, and guinea pig, with additional notes on the human lung. Am Rev Respir Dis. 1966; 94:380–387. [PubMed: 5918216]
40. Kretschmer S, Dethlefsen I, Hagner-Benes S, Marsh LM, Garn H, Konig P. Visualization of intrapulmonary lymph vessels in healthy and inflamed murine lung using cd90/thy-1 as a marker. PLoS One. 2013; 8:e55201. [PubMed: 23408960]
41. Pack RJ, Al-Ugaily LH, Morris G. The cells of the tracheobronchial epithelium of the mouse: A quantitative light and electron microscope study. J Anat. 1981; 132:71–84. [PubMed: 7275793]
42. Kistner A, Gossen M, Zimmermann F, Jerecic J, Ullmer C, Lubbert H, Bujard H. Doxycycline-mediated quantitative and tissue-specific control of gene expression in transgenic mice. Proc Natl Acad Sci U S A. 1996; 93:10933–10938. [PubMed: 8855286]
43. Krebs R, Tikkanen JM, Ropponen JO, Jeltsch M, Jokinen JJ, Yla-Herttuala S, Nykanen AI, Lemstrom KB. Critical role of vegf-c/vegfr-3 signaling in innate and adaptive immune responses in experimental obliterative bronchiolitis. Am J Pathol. 2012; 181:1607–1620. [PubMed: 22959907]
44. Bletsa A, Virtej A, Berggreen E. Vascular endothelial growth factors and receptors are up-regulated during development of apical periodontitis. J Endod. 2012; 38:628–635. [PubMed: 22515891]
45. Ni A, Lashnits E, Yao LC, Baluk P, McDonald DM. Rapid remodeling of airway vascular architecture at birth. Dev Dyn. 2010; 239:2354–2366. [PubMed: 20730909]
46. Milch RA, Rall DP, Tobie JE. Bone localization of the tetracyclines. J Natl Cancer Inst. 1957; 19:87–93. [PubMed: 13502708]
47. Deng Y, Atri D, Eichmann A, Simons M. Endothelial erk signaling controls lymphatic fate specification. J Clin Invest. 2013; 123:1202–1215. [PubMed: 23391722]
48. Mouta-Bellum C, Kirov A, Miceli-Libby L, Mancini ML, Petrova TV, Liaw L, Prudovsky I, Thorpe PE, Miura N, Cantley LC, Alitalo K, Fruman DA, Vary CP. Organ-specific lymphangiectasia, arrested lymphatic sprouting, and maturation defects resulting from gene-targeting of the pi3k regulatory isoforms p85alpha, p55alpha, and p50alpha. Dev Dyn. 2009; 238:2670–2679. [PubMed: 19705443]
49. Mettauer N, Agrawal S, Pierce C, Ashworth M, Petros A. Outcome of children with pulmonary lymphangiectasis. Pediatr Pulmonol. 2009; 44:351–357. [PubMed: 19330773]
50. Felman AH, Rhatigan RM, Pierson KK. Pulmonary lymphangiectasia. Observation in 17 patients and proposed classification. Am J Roentgenol Radium Ther Nucl Med. 1972; 116:548–558.
51. Bouchard S, Di Lorenzo M, Youssef S, Simard P, Lapierre JG. Pulmonary lymphangiectasia revisited. J Pediatr Surg. 2000; 35:796–800. [PubMed: 10813353]
52. Scalzetti EM, Heitzman ER, Groskin SA, Randall PA, Katzenstein AL. Developmental lymphatic disorders of the thorax. Radiographics. 1991; 11:1069–1085. [PubMed: 1749850]
53. Gould, SJ.; Webb, AK.; Kelsey, A. Congenital abnormalities and pediatric lung disease, including neoplasms. In: Haselton, P.; Flieder, DB., editors. Spencer's pathology of the lung. Cambridge University Press; New York: 2013. p. 66-145.
54. Allen, TC.; Cagle, PT.; Flieder, DB. Mesenchymal and miscellaneous neoplasms. In: Haselton, P.; Flieder, DB., editors. Spencer's pathology of the lung. Cambridge University Press; New York: 2013. p. 1224-1315.
55. El-Chemaly S, Malide D, Zudaire E, Ikeda Y, Weinberg BA, Pacheco-Rodriguez G, Rosas IO, Aparicio M, Ren P, MacDonald SD, Wu HP, Nathan SD, Cuttitta F, McCoy JP, Gochuico BR, Moss J. Abnormal lymphangiogenesis in idiopathic pulmonary fibrosis with insights into cellular and molecular mechanisms. Proc Natl Acad Sci U S A. 2009; 106:3958–3963. [PubMed: 19237567]
56. Das S, Ladell DS, Podgrabinska S, Ponomarev V, Nagi C, Fallon JT, Skobe M. Vascular endothelial growth factor-c induces lymphangitic carcinomatosis, an extremely aggressive form of lung metastases. Cancer Res. 2009; 70:1814–1824. [PubMed: 20179201]

57. Perl AK, Zhang L, Whitsett JA. Conditional expression of genes in the respiratory epithelium in transgenic mice: Cautionary notes and toward building a better mouse trap. Am J Respir Cell Mol Biol. 2009; 40:1–3. [PubMed: 19075182]
58. Duerr J, Gruner M, Schubert SC, Haberkorn U, Bujard H, Mall MA. Use of a new-generation reverse tetracycline transactivator system for quantitative control of conditional gene expression in the murine lung. Am J Respir Cell Mol Biol. 2011; 44:244–254. [PubMed: 20395635]
59. Anisimov A, Alitalo A, Korpisalo P, Soronen J, Kaijalainen S, Leppanen VM, Jeltsch M, Yla-Herttuala S, Alitalo K. Activated forms of vegf-c and vegf-d provide improved vascular function in skeletal muscle. Circ Res. 2009; 104:1302–1312. [PubMed: 19443835]
60. Stacker SA, Stenvers K, Caesar C, Vitali A, Domagala T, Nice E, Roufail S, Simpson RJ, Moritz R, Karpanen T, Alitalo K, Achen MG. Biosynthesis of vascular endothelial growth factor-d involves proteolytic processing which generates non-covalent homodimers. J Biol Chem. 1999; 274:32127–32136. [PubMed: 10542248]
61. Harris NC, Davydova N, Roufail S, Paquet-Fifield S, Paavonen K, Karnezis T, Zhang YF, Sato T, Rothacker J, Nice EC, Stacker SA, Achen MG. The propeptides of vegf-d determine heparin binding, receptor heterodimerization, and effects on tumor biology. J Biol Chem. 2013; 288:8176–8186. [PubMed: 23404505]
62. Ferrara N. Binding to the extracellular matrix and proteolytic processing: Two key mechanisms regulating vascular endothelial growth factor action. Mol Biol Cell. 2010; 21:687–690. [PubMed: 20185770]
63. Tammela T, He Y, Lyytikka J, Jeltsch M, Markkanen J, Pajusola K, Yla-Herttuala S, Alitalo K. Distinct architecture of lymphatic vessels induced by chimeric vascular endothelial growth factor-c/vascular endothelial growth factor heparin-binding domain fusion proteins. Circ Res. 2007; 100:1468–1475. [PubMed: 17478733]
64. Yin X, Johns SC, Lawrence R, Xu D, Reddi K, Bishop JR, Varner JA, Fuster MM. Lymphatic endothelial heparan sulfate deficiency results in altered growth responses to vascular endothelial growth factor-c (vegf-c). J Biol Chem. 2011; 286:14952–14962. [PubMed: 21343305]
65. Veikkola T, Jussila L, Makinen T, Karpanen T, Jeltsch M, Petrova TV, Kubo H, Thurston G, McDonald DM, Achen MG, Stacker SA, Alitalo K. Signalling via vascular endothelial growth factor receptor-3 is sufficient for lymphangiogenesis in transgenic mice. EMBO J. 2001; 20:1223–1231. [PubMed: 11250889]
66. Dixelius J, Makinen T, Wirzenius M, Karkkainen MJ, Wernstedt C, Alitalo K, Claesson-Welsh L. Ligand-induced vascular endothelial growth factor receptor-3 (vegfr-3) heterodimerization with vegfr-2 in primary lymphatic endothelial cells regulates tyrosine phosphorylation sites. J Biol Chem. 2003; 278:40973–40979. [PubMed: 12881528]
67. Alitalo K. The lymphatic vasculature in disease. Nat Med. 2011; 17:1371–1380. [PubMed: 22064427]
68. Olsson AK, Dimberg A, Kreuger J, Claesson-Welsh L. Vegf receptor signalling - in control of vascular function. Nat Rev Mol Cell Biol. 2006; 7:359–371. [PubMed: 16633338]
69. Tvorogov D, Anisimov A, Zheng W, Leppanen VM, Tammela T, Laurinavicius S, Holnthoner W, Helotera H, Holopainen T, Jeltsch M, Kalkkinen N, Lankinen H, Ojala PM, Alitalo K. Effective suppression of vascular network formation by combination of antibodies blocking vegfr ligand binding and receptor dimerization. Cancer Cell. 2010; 18:630–640. [PubMed: 21130043]
70. Yao LC, Baluk P, Feng J, McDonald DM. Steroid-resistant lymphatic remodeling in chronically inflamed mouse airways. Am J Pathol. 2010; 176:1525–1541. [PubMed: 20093490]
71. Carmeliet P, Jain RK. Principles and mechanisms of vessel normalization for cancer and other angiogenic diseases. Nat Rev Drug Discov. 2011; 10:417–427. [PubMed: 21629292]
72. Liao S, Liu J, Lin P, Shi T, Jain RK, Xu L. Tgf-beta blockade controls ascites by preventing abnormalization of lymphatic vessels in orthotopic human ovarian carcinoma models. Clin Cancer Res. 2011; 17:1415–1424. [PubMed: 21278244]

Novelty and Significance

What Is Known?

- Pulmonary lymphangiectasia is a life-threatening condition often evident soon after birth where respiratory function is severely impaired due to the presence of widely dilated lymphatics in the lung.
- Pulmonary lymphangiectasia is of unknown cause, and specific treatments are lacking.
- Vascular endothelial growth factor (VEGF)-C promotes the proliferation of lymphatic endothelial cells and the growth of new lymphatics.

What New Information Does This Article Contribute?

- In mice, VEGF-C overexpression in the lung resulted in pulmonary lymphangiectasia only during a critical period of perinatal development.
- Side-by-side comparison showed similarities of lymphatic abnormality in the mouse model and patients with pulmonary lymphangiectasia
- The abnormal lymphatics in mice with pulmonary lymphangiectasia resisted regression after the VEGF-C stimulus was withdrawn.

Pulmonary lymphangiectasia is a potentially lethal condition in which lung lymphatics are widely dilated and respiratory function is impaired. The condition is of unknown etiology and without specific treatment. In a ouble transgenic mouse in which VEGF-C could be switched on in the respiratory epithelium, we found an unexpected condition resembling pulmonary lymphangiectasia in human infants. Lymphangiectasia occurred only when VEGF-C was overexpressed during a critical period of perinatal development. The synergistic action of exaggerated VEGF-C mediated activation of VEGFR-2 and VEGFR-3 was required for the development of pulmonary lymphangiectasia. Abnormal lymphatic vessels persisted after the VEGF-C stimulus was withdrawn or receptor signaling was blocked. Insights from a better understanding of the cause and pathophysiology of pulmonary lymphangiectasia should lead to improved diagnostic and therapeutic approaches for this serious condition.

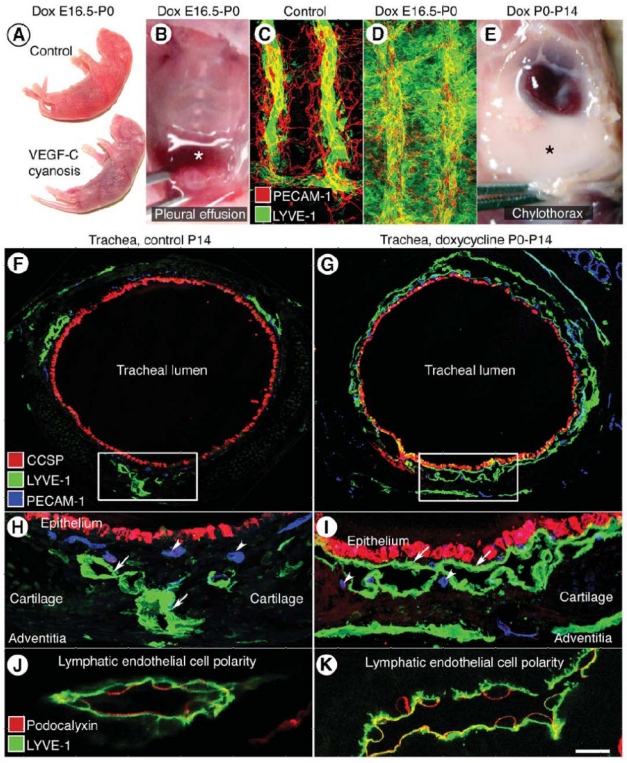

Figure 1. Lymphangiectasia in trachea of neonatal CCSP-VEGF-C mice

A, Normal skin color of control newborn mouse and cyanotic skin of newborn CCSP-VEGF-C mouse on doxycycline from E16.5 to P0. **B**, Pleural effusion (asterisk) in newborn CCSP-VEGF-C mouse on doxycycline from E16.5 to P0. **C**, Segmented pattern of lymphatics (LYVE-1, green) and blood vessels (PECAM-1, red) in normal trachea of control newborn mouse (CCSP-VEGF-C on water). **D**, Widespread lymphangiectasia in trachea of CCSP-VEGF-C mouse on doxycycline from E16.5 to P0. **E**, Chylothorax (asterisk) in CCSP-VEGF-C mouse on doxycycline from P0 to P14. **F-I**, Tracheal cross-sections stained for epithelial Clara cells (CCSP, red), lymphatics (LYVE-1 green), and blood vessels (PECAM-1, blue) in CCSP-VEGF-C mice on water (**F, H)** or doxycycline (**G, I**) from P0 to P14. **F**, Lymphatics in control mouse are scattered around the trachea. **G**, Lymphatics in CCSP-VEGF-C mouse on doxycycline surround most of the trachea beneath the epithelium. Boxes in **F** and **G** mark regions in **H** and **I** that show the differences in lymphatics (LYVE-1, green, arrows) and similarities of blood vessels (PECAM-1, blue, arrowheads) in the two conditions. **J-K**, Podocalyxin (red) is restricted to the luminal surface and LYVE-1 (green) is on both surfaces of lymphatic endothelium in CCSP-VEGF-C mice on water (**J**) or doxycycline (**K**) from P0 to P14, demonstrating that lymphatic sacs in lymphangiectasia have a lumen (**K**). Scale bar: 100 μm (**C-D**); 150 μm (**F-G**); 50 μm (**H-I**); 10 μm (**J-K**).

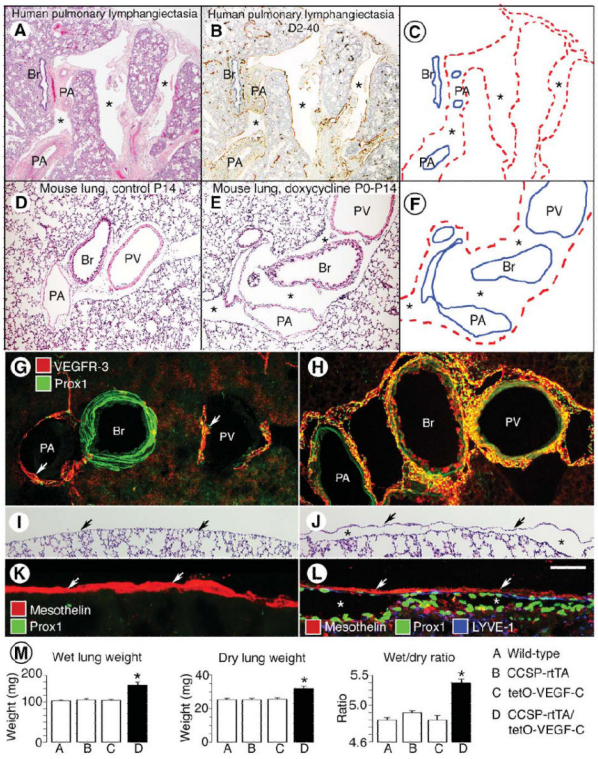

Figure 2. Comparison of lungs in child with pulmonary lymphangiectasia and in neonatal CCSP-VEGF-C mice

A-B, Widely dilated lymphatics (asterisks) in lung from a 1-month-old girl with pulmonary vein stenosis accompanied by lymphangiectasia (Case A). Sections from autopsy specimen stained by H&E (**A**) or D2-40/podoplanin (**B,** brown). **C**, Enlarged lymphatics in A and B are marked by dashed red lines. Other landmarks are shown by solid blue lines. Br, bronchiole; PA, pulmonary artery; and PV, pulmonary vein. **D-E**, Lung sections stained by H&E from neonatal CCSP-VEGF-C mice on water (**D**) or doxycycline (**E**) from P0 to P14. **F**, Regions of lymphangiectasia in E (asterisks) around bronchi and pulmonary vessels are outlined by dashed red lines. **G-H**, Sparse lymphatics around major bronchus and pulmonary vessels (arrows) in lung of control mouse on water (**G**) compared to widespread lymphatics in lung of CCSP-VEGF-C mouse on doxycycline from P0 to P14 (**H**). Sections stained for VEGFR-3 (red) and Prox1 (green). Green staining of bronchial smooth muscle does not reflect Prox1. **I-J**, Lung section with no pleural lymphatics in neonate on water (**I**) compared to subpleural lymphangiectasia (asterisks) in lung of neonate on doxycycline from P0 to P14 (**J**). Arrows mark surface of visceral pleura. Stained by H&E. **K-L**, Visceral pleura stained for mesothelin (red, arrows) has no lymphatics in control lung (**K**) but overlies subpleural lymphangiectasia (Prox1, green nuclei, asterisks) in lung of CCSP-VEGF-C mouse on doxycycline (**L**). **M**, Measurements of wet lung weight (mg), dry lung weight (mg), and ratio of wet-to-dry lung weight for wild-type mice (A), single transgenic mice (B, C), and CCSP-VEGF-C double transgenic mice on doxycycline from P0 to P35 (D). All three measurements in CCSP-VEGF-C mice are abnormal. *$P < 0.05$ vs. wild-type. Scale bar: 250 μm (**D-E**); 150 μm (**G-J**); 50 μm (**K-L**).

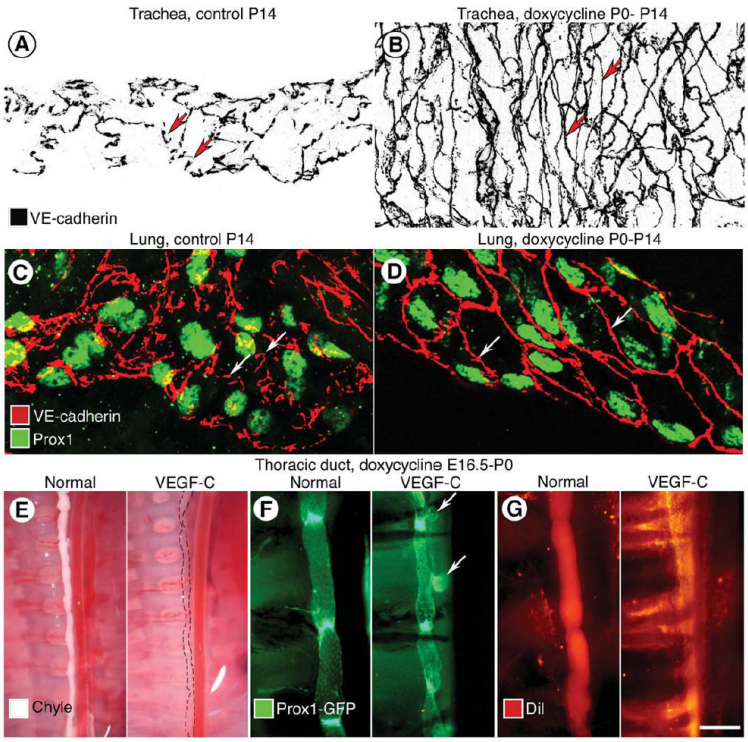

Figure 3. Abnormal lymphatic junctions and barrier function in lymphangiectasia

A-B, Adherens junctions (VE-cadherin, black) between endothelial cells of tracheal lymphatics are shown in inverted grayscale images. Discontinuous, button-like junctions (arrows) in lymphatic of normal mouse at P14 (**A**) are contrasted with continuous zipper-like junctions (arrows) in lymphatic of CCSP-VEGF-C mouse on doxycycline from P0 to P14 (**B**). **C-D**, Adherens junctions (VE-cadherin, red) between endothelial cells of lung lymphatics (Prox1, green), compare button-like junctions (arrows) in CCSP-VEGF-C mouse on water (**C**) with zipper-like junctions (arrows) in mouse on doxycycline from P0 to P14 (**D**). **E-G**, Image pairs comparing thoracic duct in normal Prox1-GFP mouse at P0 and Prox1-GFP/CCSP-VEGF-C mouse on doxycycline from E16.5 to P0. **E**, Thoracic duct normally filled with chyle (left) is compared to almost invisible thoracic duct in mouse on doxycycline (dashed lines, right). **F**, Thoracic duct with strong Prox1-GFP fluorescence in normal valves (left) is compared to thoracic duct with herniations (arrows) and abnormal valves in mouse on doxycycline (right). **G**, Normal thoracic duct filled with DiI-labeled chyle from milk (left) is compared to DiI extravasated from thoracic duct in mouse on doxycycline. Scale bar: 20 μm (**A-D**); 900 μm (**E**); 250 μm (**F-G**).

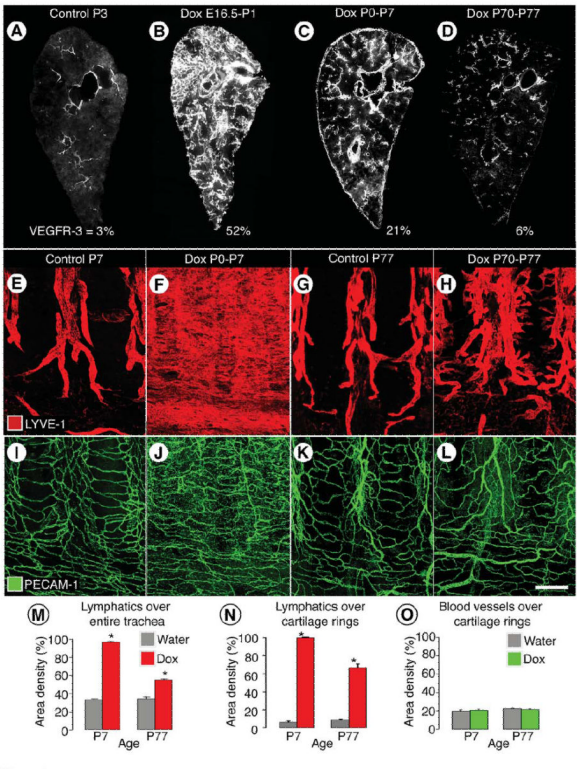

Figure 4. Age-related decrease in severity of VEGF-C driven lymphangiectasia

A-D, Decreased severity of lymphangiectasia in CCSP-VEGF-C mice on doxycycline beginning at E16.5, P0, or P70. Photographic montages of lungs showing age-related differences in abundance of lymphatics (VEGFR-3 immunoreactivity, white), and corresponding area densities of white pixels (%), in CCSP-VEGF-C mice on water at P3 (**A**) or on doxycycline from E16.5 to P1 (**B**), P0 to P7 (**C**), or P70 to P77 (**D**). **E-L,** Lymphatics (E-H, LYVE-1, red) and blood vessels (I-L, PECAM-1, green) in tracheal whole mounts from newborn (**E, F, I, J**) and adult (**G, H, K, L**) CCSP-VEGF-C mice on water (**E, G, I, K**) or doxycycline (**F, H, J, L**) for 7 days. **E, G**, Segmented pattern of lymphatics in neonatal and adult mice on water. **F**, Sheet-like lymphangiectasia in neonatal mouse on doxycycline from P0 to P7. **H**, Sprouting lymphangiogenesis in adult mouse on doxycycline from P70 to P77. **I-L**, No apparent differences in blood vessels of neonatal or adult mice on water or doxycycline. **M-O**, Area density of lymphatics over entire trachea (**M**), over cartilage rings (**N**), and corresponding blood vessels over cartilage rings (**O**). * $P < 0.05$ vs. water. Scale bar: 450 μm (**A, C**); 350 μm (**B**); 600 μm (**D**)**;** 200 μm (**E-L**).

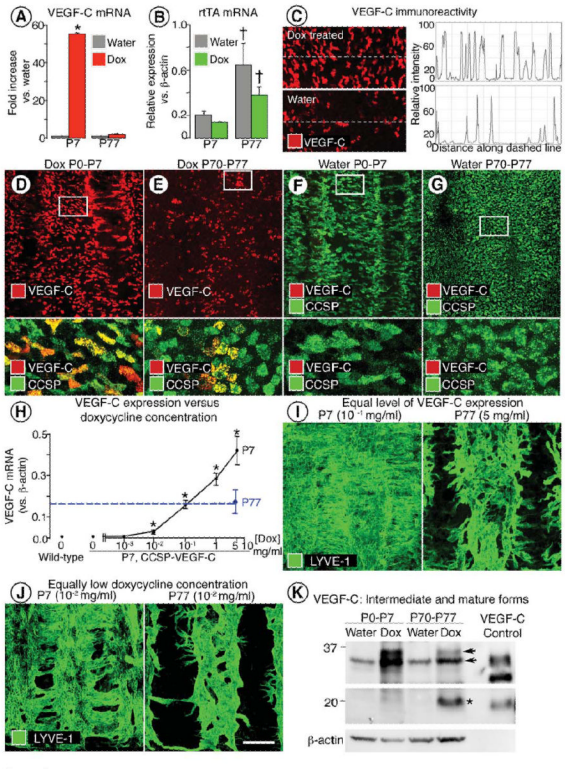

Figure 5. VEGF-C comparison in neonatal and adult CCSP-VEGF-C mice

A-B, VEGF-C (**A**) and rtTA (**B**) mRNA expression in trachea of CCSP-VEGF-C mice at P7 or P77 after doxycycline for 7 days and in corresponding controls (water). **P* < 0.05 vs. neonates on water; †*P* < 0.05 vs. neonates on water or doxycycline. **C**, Intensity of VEGF-C immunofluorescence, measured along dashed line with ImageJ, in tracheal epithelium imaged by confocal microscopy with the same settings. **D-G**, VEGF-C immunoreactivity (red) in epithelium of tracheal whole mounts of neonatal and adult mice shown alone (**D, E**, upper) and with CCSP (green) immunoreactivity. White boxes in **D-G** demarcate regions enlarged below. **H**, Dose-response relationship between VEGF-C mRNA expression in trachea and doxycycline concentration in drinking water. Tracheal VEGF-C mRNA was about the same (dashed line) in neonates on doxycycline at 10^{-1} mg/ml and adults on doxycycline at 5 mg/ml. * *P* < 0.05 vs. water (0 on X-axis; 0.005 on Y-axis). **I**, Lymphangiectasia (LYVE-1) occurred in neonates but not in adults even when doxycycline concentration was adjusted to match VEGF-C expression at the two ages. **J**, Similarly, lymphangiectasia was present in neonates but not in adults when both were given doxycycline at a low concentration (10^{-2} mg/ml). **K**, Western blot showing stronger bands for intermediate forms of VEGF-C (32-35 kDa) in neonates than in adults on doxycycline for 7 days (upper panel). The mature form of VEGF-C (20 kDa, asterisk) is more abundant in adults on doxycycline (middle panel). Bands from conditioned medium harvested from cells transfected with native mouse VEGF-C serve as a reference for molecular weights [59]. The products of full-length cDNA contain intermediate and mature forms of VEGF-C polypeptides. Intermediate forms from CCSP-VEGF-C mice are slightly larger in molecular weight than the corresponding positive control. Upper and middle panels are from different exposures of the same blot. Loading control is beta-actin (lower panel). Scale bar: 70 μm (**C**); 125 μm (**D-G** upper; **I-J** left); 25 μm (**D-G** lower); 175 μm (**I-J** right).

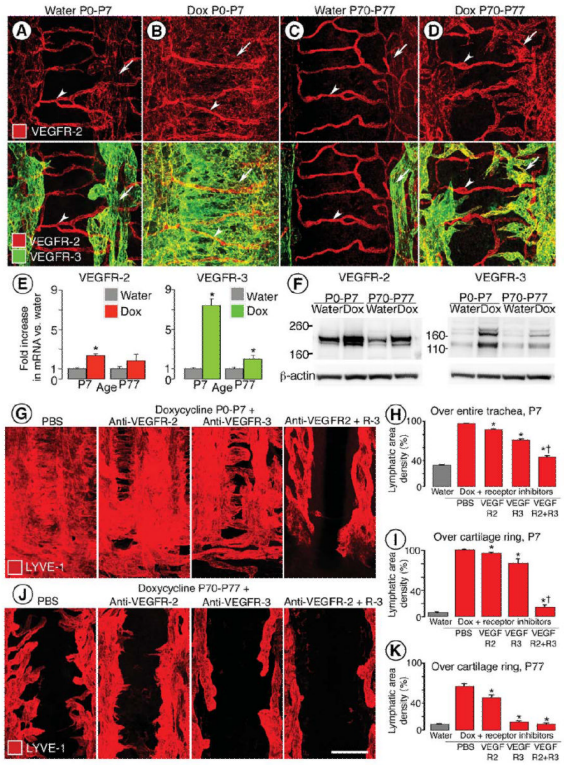

Figure 6. VEGFR-2 and VEGFR-3 in trachea of CCSP-VEGF-C mice

A-D, Strong VEGFR-2 immunoreactivity (red) in tracheal blood vessels (arrowheads) and weak VEGFR-2 staining in lymphatics (arrows) compared to strong VEGFR-3 staining in lymphatics of CCSP-VEGF-C mice on water or doxycycline from P0 to P7 or P70 to P77. **E**, Expression of VEGFR-2 and VEGFR-3 mRNA in trachea of same groups as in A-D (N = 8 per group). *$P < 0.05$ vs. baseline at corresponding age. **F**, Western blots for VEGFR-2 and VEGFR-3 in trachea of same groups as in **E** (N = 10 per group). Loading control is beta-actin. In neonates, VEGFR-2 protein was increased 2-fold and VEGFR-3 was increased 7-fold after doxycycline. In adults, VEGFR-2 protein was increased 2-fold and VEGFR-3 was increased 4-fold after doxycycline. **G, J**, Lymphatics stained for LYVE-1 (red) in tracheal whole mounts of neonatal (**G**) or adult (**J**) mice after doxycycline plus PBS, anti-VEGFR-2 antibody DC101, anti-VEGFR-3 antibody mF4-31C1, or both antibodies for 7 days. Scale bar: 80 μm (**A-D**); 200 μm (**G, J**). **H, I, K**, Extent of inhibition of lymphangiogenesis in CCSP-VEGF-C mice treated with doxycycline and inhibitory antibodies used in **G** and **J**. LYVE-1-positive lymphatics were assessed over entire trachea of neonatal mice at P7 (**H**) or by measuring sprouts over cartilage rings at P7 (**I**) or P77 (**K**). * $P < 0.05$ vs. PBS. † $P < 0.05$ vs. mF4-31C1.

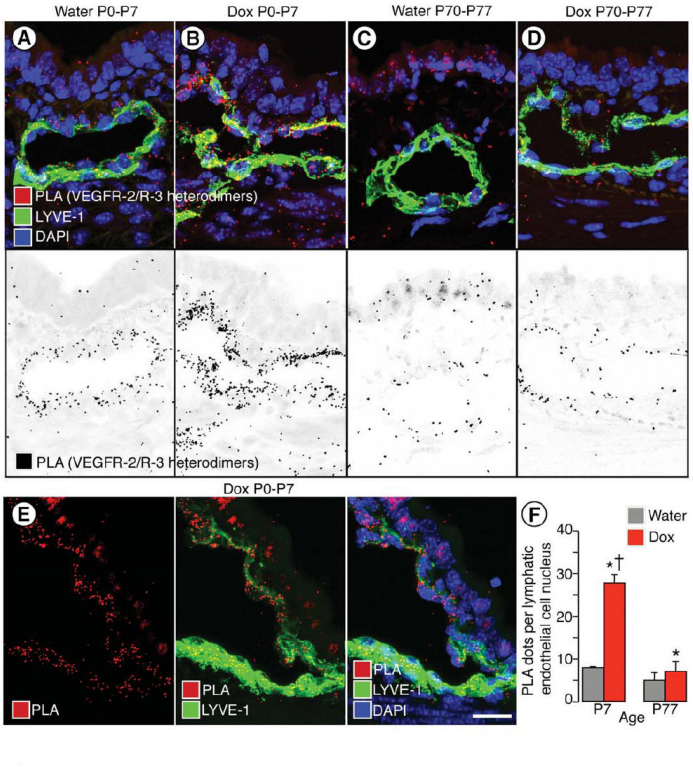

Figure 7. VEGFR-2/VEGFR-3 heterodimers revealed in lymphatic endothelial cells by proximity ligation assay (PLA)

A-D, Confocal micrographs comparing the number of PLA red dots (VEGFR-2/VEGFR-3 heterodimers) in tracheal lymphatics (LYVE-1, green) of neonatal (**A-B**) and adult (**C-D**) CCSP-VEGF-C mice on water or doxycycline for 7 days. Nuclei are stained with DAPI. Inverted grayscale versions of the same images emphasize the larger number of PLA dots in the neonate (**B**, lower) than in the adult (**D,** lower). **E**, PLA dots marking lymphatic endothelial cells in trachea of neonatal CCSP-VEGF-C mouse on doxycycline for 7 days, shown alone (left panel), with LYVE-1 (middle panel), and with LYVE-1 and DAPI-stained nuclei (right panel). Scale bar: 20 μm. **F**, Number of PLA dots per lymphatic endothelial cell nucleus. *$P < 0.05$ vs. water; †$P < 0.05$ vs. adults on doxycycline.

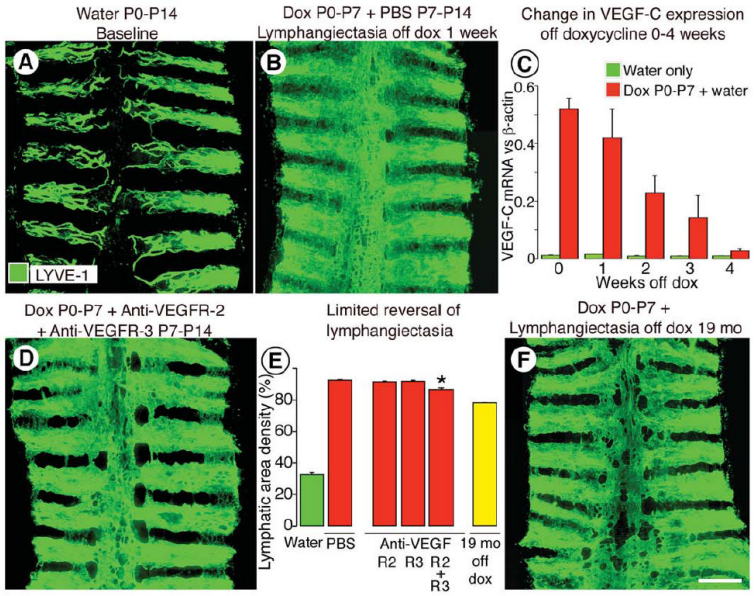

Figure 8. Limited reversibility of lymphangiectasia

A-B, Lymphatics stained for LYVE-1 immunoreactivity in tracheal whole mounts from CCSP-VEGF-C mice at baseline (**A**) or after doxycycline from P0 to P7 and then no doxycycline from P7 to P14 (**B**). Lymphangiectasia is still widespread after one week off doxycycline. **C**, Expression of VEGF-C mRNA in trachea of CCSP-VEGF-C mice ($N = 5$ per group) at baseline (green) or after doxycycline from P0 to P7 and then no doxycycline for 0 to 4 weeks (red). **D, E**, Extent of lymphangiectasia in trachea shown by LYVE-1 staining after doxycycline from P0 to P7 followed by inhibition of VEGFR-2, VEGFR-3, and both receptors by DC101 or mF4-31C1 given from P7 to P14 (**D**). Area density of LYVE-1 immunoreactivity over the entire trachea under these conditions (**E**). * $P < 0.05$ vs. PBS. **F**, Persistence of lymphangiectasia in trachea of a mouse on doxycycline from P0 to P7 and then off doxycycline for 19 months. Amount at 19 months (**E**, yellow bar) is only 24% less than at P7. Scale bar: 450 μm (**A-B, D**); 700 μm (**F**).